Journal of Oceanology and Limnology

https://doi.org/10.1007/s00343-026-5484-y

Research Paper

Remote sensing observation of algal bloom encroachment into aquatic vegetation in Taihu Lake over the past two decades*

Chen GUO[1, 2], Junfeng XIONG[2, **], Jinyi HUANG[2], Man HOU[1, 2], Xudong ZHOU[3], Chen LIN[2], Ronghua MA[2, 4], Yang XIANG[1]

[1] *College of Geomatics, Xi' an University of Science and Technology, Xi' an 710054, China*

[2] *State Key Laboratory of Lake and Watershed Science for Water Security, Nanjing Institute of Geography and Limnology, Chinese Academy of Sciences, Nanjing 211135, China*

[3] *School of Civil & Environmental Engineering and Geography Science, Ningbo University, Ningbo 315211, China*

[4] *University of Chinese Academy of Sciences, Nanjing 211135, China*

Received Nov. 27, 2025; accepted in principle Dec. 26, 2025; accepted for publication Feb. 12, 2026

Abstract Taihu Lake is one of the most severely eutrophic large lakes worldwide, characterized by a complex ecosystem where algal blooms and aquatic vegetation coexist, and it serves as a critical regional water source. Identifying the channels through which algal blooms invade vegetated areas and understanding their underlying mechanisms is essential for effective lake management. In this study, multi-source remote-sensing data were used to extract the spatial patterns of algal bloom frequency and aquatic vegetation over the past 22 years. We detected the major encroachment routes of algal blooms into vegetated zones and revealed the long-term interaction mechanisms between algae and vegetation. Algal blooms were persistently concentrated in the western and northern bays, exhibiting an overall fluctuating upward trend. Aquatic vegetation was mainly distributed in four eastern bays, remained relatively stable before 2015, declined markedly in 2016 due to dredging and shoreline modifications, and then gradually recovered. A stable negative response relationship was observed between algal blooms and aquatic vegetation, jointly regulated by seasonal climate and nutrient structure. High temperatures and intense precipitation in summer facilitated bloom expansion, whereas low temperatures in winter favored vegetation recovery. Meanwhile, lower TN to TP ratios suppressed vegetation growth and enhanced bloom encroachment during summer. Three primary channels of algal bloom encroachment into vegetated areas were identified: the northern shoreline of Gonghu Bay, the surroundings of Dongshan Island, and the southern marginal zone. Among them, the water intake in northern Gonghu Bay represents the most vulnerable zone requiring priority control. Although bloom risk is relatively low for the central and southern water intakes, maintaining the existing hydrodynamic regime and vegetation structure remains essential to prevent vegetation degradation, and enhanced monitoring is needed to identify in situ bloom occurrences within vegetated regions.

Keyword: algal bloom; aquatic vegetation; Taihu Lake; remote sensing

1 INTRODUCTION

In lake ecosystems, algal blooms and aquatic vegetation are two key groups of primary producers whose spatial distribution and interactions play a crucial role in regulating ecological balance and water quality (Hilt et al., 2018; Paerl et al., 2011). Aquatic vegetation stabilizes sediments, absorbs excess nutrients, and improves water transparency, thereby supporting ecosystem functioning and water

* Supported by the National Key R&D Program of China (No. 2021YFD1700600), the Natural Science Foundation of Jiangsu Province (No. BK20240113), the National Natural Science Foundation of China (Nos. 42361144002, 42201400), and the Jiangsu Natural Resources Science and Technology Innovation Program (No. JSZRKJ202409)

** Corresponding author: jfxiong@niglas.ac.cn

purification (Zhu et al., 2015; Zeng et al., 2017). In eutrophic lakes, however, recurrent algal blooms frequently occur and exhibit complex coexistence and competition with aquatic vegetation, influencing nutrient cycling, light availability, and habitat stability in shallow-water systems (Li et al., 2009; Bilous et al., 2023; Liu et al., 2024). Understanding bloom-vegetation interactions is therefore essential for eutrophication control and aquatic ecosystem restoration (Duan et al., 2009).

Previous studies have shown that aquatic vegetation can suppress algal growth through shading, nutrient uptake, and allelopathic effects (Li et al., 2009; Bilous et al., 2023). Under eutrophic conditions or during high-biomass blooms, however, these inhibitory effects may weaken or reverse, leading to reduced growth or loss of submerged plants (Liu et al., 2024). Nutrient loading and vegetation coverage jointly regulate the competitive balance between algae and macrophytes, thereby controlling bloom frequency and intensity (Xie et al., 2013; Zhu et al., 2015; Zeng et al., 2017; Hilt et al., 2018; Iacarella et al., 2018). Some studies have found that transitions between vegetation-dominated and phytoplankton-dominated states have been reported, with water transparency, nutrient availability, and temperature acting as key regulators (Zhang et al., 2019; Wang et al., 2020).

Taihu Lake, a large eutrophic shallow lake located in the Changjiang (Yangtze) River Delta, provides a representative natural system for examining these interactions. The lake is shallow, nutrient-rich, and strongly influenced by wind-driven hydrodynamics, making it highly susceptible to recurrent algal blooms (Qin et al., 2007; Duan et al., 2009). Pronounced spatial heterogeneity characterizes the lake: the western and northern bays (e.g., Meiliang Bay, Zhushan Bay, and Gonghu Bay) are persistent bloom hotspots, whereas the eastern lake is dominated by submerged and emergent vegetation, forming a relatively clear-water ecosystem (Zhao et al., 2017; Yang et al., 2021). Blooms typically originate in nutrient-enriched northwestern regions and are transported eastward under prevailing winds, leading to recurrent bloom intrusion into vegetation-dominated areas (Zhang et al., 2019; Chen et al., 2020). In this context, eastern Taihu functions as an ecological buffer zone, where aquatic vegetation plays a critical role in mitigating bloom expansion by intercepting nutrients, attenuating light, and reducing sediment resuspension (Zhu et al., 2015; Zeng et al., 2017).

Although advances in remote sensing-based monitoring of algal blooms and aquatic vegetation, most studies have treated these components independently, focusing on their individual distribution patterns or temporal trends (Hu, 2009). Lake-wide, long-term analyses explicitly addressing bloom intrusion into aquatic vegetation zones remain scarce. Moreover, current ecological understanding of bloom-vegetation competition is largely derived from localized field observations or short-term experiments (Li et al., 2009; Hilt et al., 2018), limiting the ability to identify persistent spatial pathways and long-term encroachment dynamics at the whole-lake scale. Given the long-term coexistence of extensive algal blooms and large aquatic vegetation zones in Taihu Lake, this lake provides an ideal natural system to address these gaps. Using long-term remote sensing observations, this study identifies the spatial channels through which algal blooms repeatedly expand into vegetation-dominated areas and examines their seasonal to interannual dynamics and potential drivers at the lake-wide scale.

In Taihu Lake, algal blooms are primarily concentrated in the western lake, whereas aquatic vegetation is mainly distributed in the eastern region (Qin et al., 2007; Zhao et al., 2013). Driven by wind forcing and other environmental factors, blooms originating from the western lake can expand eastward and repeatedly intrude into vegetation-dominated areas, where they compete with aquatic vegetation for light and nutrient resources (Duan et al., 2009; Li et al., 2009; Chen et al., 2020; Xue et al., 2023). Therefore, the encroachment of algal blooms into aquatic vegetation zones, accompanied by competition for available resources, has been regarded as an encroachment phenomenon in previous studies. In this study, the intensity of algal bloom encroachment is characterized using the frequency and areal extent of bloom occurrence within aquatic vegetation areas derived from remote sensing observations.

Accordingly, "bloom encroachment" refers to the persistent and directional expansion of algal bloom occurrence from algal-dominated regions into aquatic vegetation-dominated areas, as inferred from long-term satellite observations (Scheffer et al., 1993, 2001). It does not imply direct biological encroachment, ecological replacement, or explicitly resolved physical transport processes. Instead, encroachment here denotes a long-term spatial pattern characterized by increasing bloom frequency, aggregation, and recurrence within vegetation zones, beyond short-term co-occurrence or transient overlap.

The objectives of this study are to:

(1) Characterize long-term coexistence and competition between algal blooms and aquatic vegetation using multi-decadal remote sensing data.

(2) Identify bloom encroachment channels into vegetated regions to support region-specific water-security and ecosystem management strategies.

2 MATERIAL AND METHOD

2.1 Study area

Taihu Lake, the third-largest freshwater lake in China, is located in the core region of the Changjiang River Delta (30°55′40″N–31°32′58″N, 119°52′32″E–120°36′10″E). It is a typical shallow and eutrophic lake, with a maximum depth of 2.6 m and an average depth of 1.9 m, providing favorable conditions for the growth of phytoplankton and aquatic vegetation. Historically, a total of 14 dominant aquatic plant species have been identified in Taihu Lake (Lei, 2006), mainly distributed in the eastern bays (Regions 2, 3, and 4), which are commonly recognized as vegetation-dominated areas (Zhao et al., 2012, 2013; Luo et al., 2014). Harmful algal blooms are primarily concentrated in the northern and western regions, including Meiliang Bay, Zhushan Bay, Gonghu Bay, and the western shoreline (Duan et al., 2009). Driven by wind and water currents, these blooms can drift and expand toward eastern Taihu Lake, invading the zones dominated by aquatic vegetation (Zhang et al., 2019). In this region, seven major water intakes serving more than ten million residents are located along the lakeshore (Fig.1). The frequent intrusion of algal blooms has thus become a significant threat to the water environment and the safety of regional drinking water supplies.

2.2 Overall analytical workflow

To investigate the long-term interactions between algal blooms and aquatic vegetation in Taihu Lake, this study integrates multi-source remote sensing data with spatial statistical and environmental analyses. The overall analytical workflow is summarized in Fig.2, which includes data acquisition and preprocessing, bloom-vegetation interaction analysis, and application-oriented risk assessment. The detailed methods are described in the following sections.

The framework consists of three main components:

(1) data acquisition and preprocessing using multi-source remote sensing, meteorological, and nutrient datasets;

(2) bloom-vegetation interaction analysis, including bloom and vegetation extraction, encroachment

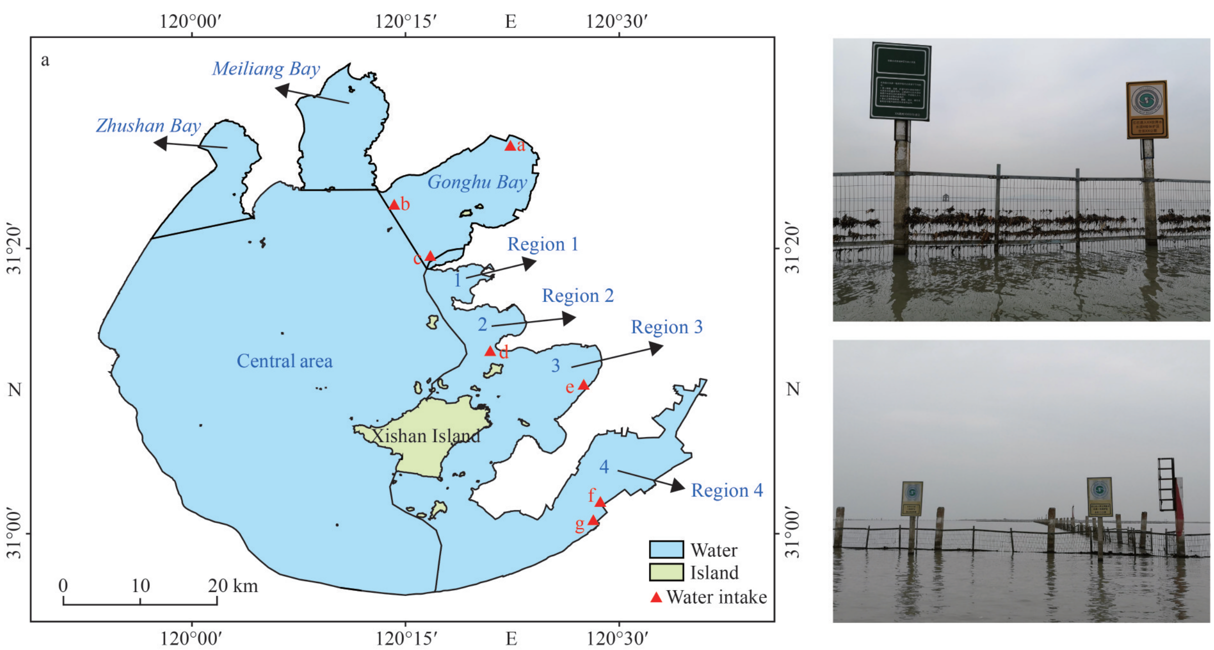

Fig.1 Overview of the research area and on-site photos of the water intake point

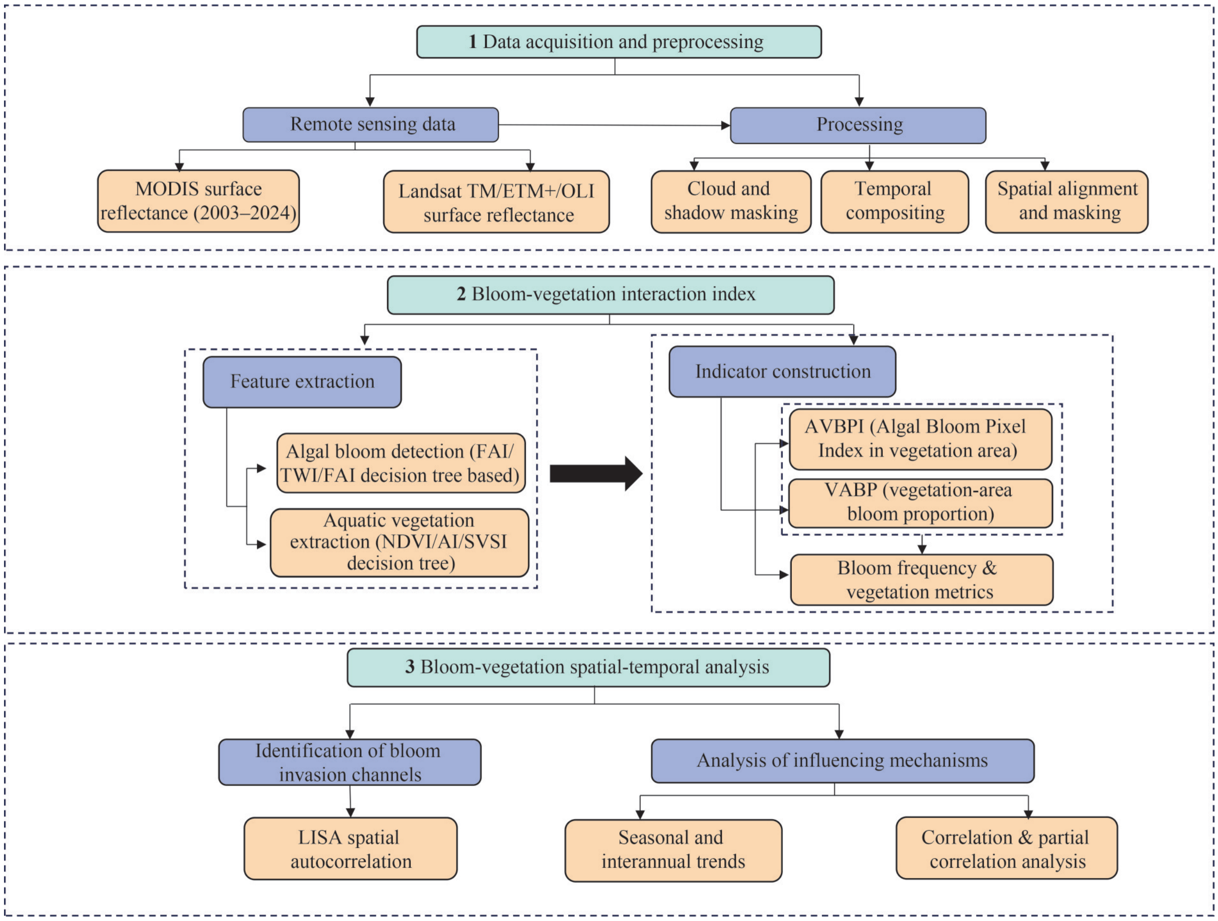

Fig.2 Overall workflow of the study

metrics construction (AVBPI and VABP), spatiotemporal analysis, and environmental relationship assessment;

(3) risk assessment and management implications focusing on intake-based bloom risk and region-specific mitigation strategies.

2.3 Remote sensing data acquisition and preprocessing

To ensure consistency with the temporal sequence of the study, MOD09GA surface reflectance data from 2003 to 2024 were used to identify algal bloom occurrence in Taihu Lake. The MOD09GA product provides daily gridded Level-2G (L2G) surface reflectance data across seven spectral bands (Bands 1–7). The preprocessing steps included cloud removal, reflectance conversion, and band selection, while retaining the original time-series information of the images. The frequency of algal bloom occurrence was calculated by counting the number of times each pixel was identified as a bloom pixel throughout the time series and dividing it by the total number of valid observations.

To correspond with the MODIS-based bloom time series and obtain accurate spatial information of aquatic vegetation, Landsat 5 TM, Landsat 7 ETM+, and Landsat 8 OLI Level-2 surface reflectance (SR) datasets were used to extract aquatic vegetation in Taihu Lake. Image preprocessing was conducted on the Google Earth Engine (GEE) platform. Since many images contained cloud and cloud-shadow pixels, the Quality Assessment (QA) band was used to detect and mask contaminated pixels. Only images with less than 20% cloud cover were retained, and median compositing was applied to fill missing pixels and generate temporally continuous vegetation datasets.

Previous studies have demonstrated that Landsat TM, ETM+, and OLI sensors exhibit high radiometric and spectral consistency after standard atmospheric correction, ensuring the continuity and comparability of long-term Landsat time series (Roy et al., 2014, 2016; Markham et al., 2015). In addition, Landsat-8 OLI data have been shown to be largely compatible with Landsat TM/ETM+ for inland water and aquatic vegetation applications, with cross-sensor differences generally small relative to long-term spatial and temporal patterns (Pahlevan et al., 2017).

Algal blooms and aquatic vegetation were retrieved independently from MODIS and Landsat data, respectively, and all subsequent analyses were conducted within the native spatial resolution of each dataset.

2.4 Algal bloom frequency

2.4.1 Model construction

In this study, the decision tree classification method proposed by Liang et al. (2017) was employed to identify algal blooms in Taihu Lake. The method determines optimal index thresholds to filter target pixels and calculates the proportion of pixels that meet the criteria, thereby obtaining the occurrence frequency of algal blooms across different seasons. The technical workflow is shown in Fig.3.

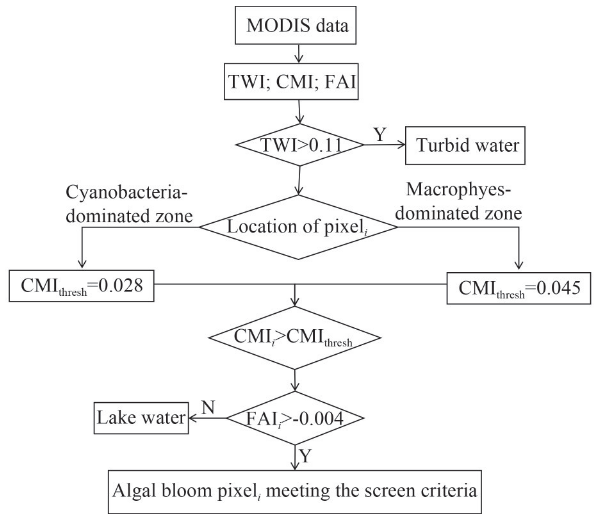

Fig.3 Decision tree model used for extracting algal bloom based on multi-index threshold classification

Using MODIS satellite imagery, pixel-by-pixel calculations were performed to derive three spectral indices: the Turbid Water Index (TWI), the Cyanobacteria-Macrophyte Index (CMI), and the Floating Algae Index (FAI). Pixels with TWI>0.11 were classified as turbid-water areas with high suspended sediment concentrations and were excluded from further bloom identification.

For macrophyes-dominated zone, bloom pixels were identified using the thresholds CMI>0.028 and FAI>-0.004, while pixels below these thresholds were classified as non-bloom water. For cyanobacteria-dominated zone, the bloom detection thresholds were CMI>0.045 and FAI>-0.004. Pixels that did not meet these criteria were classified as open water. According to previous studies (Zhao et al., 2012, 2013; Luo et al., 2014), the eastern region of Taihu Lake was defined as the macrophyte-type zone, whereas the western and central regions were defined as cyanobacteria-dominated zone. The indicators presented in Fig.3 are listed in Table 1.

2.5 Aquatic vegetation identification

2.5.1 Model construction

The aquatic vegetation in eastern Taihu Lake was identified following the model proposed by Yang et al. (2021). In their study, the Emergent Vegetation Sensitive Index (EVSI) was constructed using the narrow near-infrared (Band 8a) of Sentinel-2, which is highly sensitive to emergent vegetation. Since the present study employed Landsat imagery rather than Sentinel-2 data, and because the Landsat near-infrared band has a similar wavelength range to Sentinel-2 Band 8a, the Normalized Difference Vegetation Index (NDVI) was used to identify emergent vegetation. To further improve the discrimination among different water surface types, the Algae Index (AI) and the Submerged Vegetation

Table 1 Indices for algal bloom extraction in Taihu Lake

Index name	Mathematical expression	Functional application
Algal Bloom and Aquatic Vegetation Discrimination Index (CMI) (Liang et al., 2017)	$\mathrm{CMI} = R_{\mathrm{GREEN}} - R_{\mathrm{BLUE}} - \left[R_{\mathrm{SWIR}} - R_{\mathrm{BLUE}}\right] \times \frac{(\lambda_{\mathrm{GREEN}} - \lambda_{\mathrm{BLUE}})}{\lambda_{\mathrm{SWIR}} - \lambda_{\mathrm{BLUE}}}$	Discriminates between bloom waters and aquatic vegetation-dominated waters
Floating Algae Index (FAI) (Hu et al., 2010)	$\mathrm{FAI} = R_{\mathrm{NIR}} - R_{\mathrm{RED}} - \left[R_{\mathrm{SWIR}} - R_{\mathrm{RED}}\right] \times \frac{(\lambda_{\mathrm{NIR}} - \lambda_{\mathrm{RED}})}{\lambda_{\mathrm{SWIR}} - \lambda_{\mathrm{RED}}}$	Identifies floating algae via remote sensing techniques
Turbid Water Index (TWI) (Feng et al., 2012)	$\mathrm{TWI} = R_{\mathrm{RED}} - R_{\mathrm{SWIR}}$	Eliminates pixels of water bodies with high suspended solids, thereby enhancing the monitoring precision of CMI and FAI

R_{GREEN}, R_{BLUE}, $\mathrm{R}_{\mathrm{SWIR}}$, R_{NIR}, and R_{RED} denote the reflectance values of the corresponding spectral bands. λ_{GREEN}, λ_{BLUE}, λ_{SWIR}, λ_{NIR}, λ_{RED} represent the central wavelengths of the respective bands.

Sensitive Index (SVSI) were integrated into the classification framework.

Based on the combination of these spectral indices, aquatic vegetation and algal blooms were effectively separated from open water. Pixels with NDVI>0.5 were identified as emergent vegetation, those with AI≥0.035 were classified as algal blooms, and those with SVSI<2 400 were recognized as submerged vegetation. According to these criteria, emergent and submerged vegetation were extracted separately and subsequently merged to generate the overall spatiotemporal distribution of aquatic vegetation in Taihu Lake. The calculation formulas for NDVI, AI, and SVSI are summarized in Table 2, and the corresponding index maps are shown in Fig.4.

2.5.2 Accuracy assessment

The classification accuracy of aquatic vegetation extraction in Taihu Lake was evaluated using high-resolution Google Earth imagery as reference data. For each of the three Landsat sensors (TM, ETM+, and OLI), 95 independent validation points were randomly selected for the corresponding time periods (Fig.5). A confusion matrix was constructed to assess the consistency between the remote sensing classification results and the ground reference data (Table 3), following the "predicted class (rows)×actual class (columns)" format (Foody, 2002).

The evaluation metrics included true positive (TP), false positive (FP), false negative (FN), and true negative (TN). Based on the confusion matrix, several accuracy indicators were calculated, including overall accuracy (OA), user's accuracy (UA), producer's accuracy (PA), and the Kappa coefficient (Pontius and Millones, 2011). These indices provide a comprehensive assessment of the classification reliability and the spatial agreement between extracted vegetation maps and reference data.

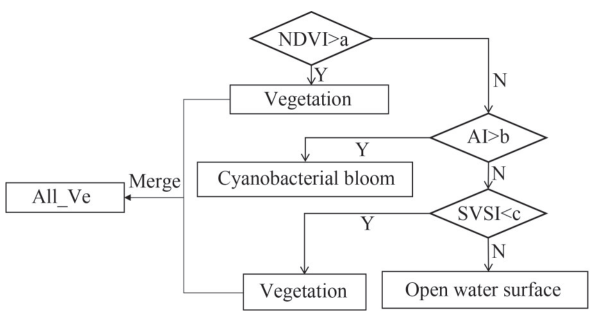

Fig.4 Decision tree model used for extracting aquatic vegetation based on multi-index threshold classification

2.6 Overlap area extraction

Before defining the encroachment-related indices, two basic spatial metrics are introduced.

AVA (aquatic vegetation area) refers to the total area classified as aquatic vegetation within the study region during a given period, derived from Landsat-based vegetation maps.

ORA (overlap area) represents the spatial overlap between algal bloom pixels and aquatic vegetation pixels, indicating areas where algal blooms occur within vegetation-dominated zones at a given time.

On this basis, two encroachment-related indices were further developed to more intuitively characterize the encroachment intensity of algal blooms within aquatic vegetation zones.

It should be noted that aquatic vegetation and algal blooms were extracted independently based on their respective satellite datasets. Therefore, the encroachment-related indices defined below are calculated within the native spatial resolution of each product and are based on pixel-level frequency and proportion statistics rather than exact geometric area matching. As a result, differences in spatial resolution between MODIS and Landsat do not affect the internal consistency of these indices. Potential mixed-pixel effects are mainly confined to vegetation-water boundary zones and are expected to have a limited influence on the long-term, regional-scale patterns emphasized in this study.

(1) The Algal Bloom Pixel Index in Vegetation Area (AVBPI)

$$\mathrm{AVBPI}_i = \frac{T_{\mathrm{cya}\text{-}i}}{T_{\mathrm{val}\text{-}i}} \times 100\%. \tag{1}$$

Table 2 Indices for aquatic vegetation and algal bloom discrimination

Index name	Mathematical expression	Functional application
Normalized Difference Vegetation Index (NDVI)	$\mathrm{NDVI} = \frac{B_{\mathrm{NIR}} - B_{\mathrm{RED}}}{B_{\mathrm{NIR}} + B_{\mathrm{RED}}}$	Distinguish emergent vegetation from algal blooms
Algal Index (AI)	$\mathrm{AI} = B_{\mathrm{GREEN}} - \frac{B_{\mathrm{BLUE}} + B_{\mathrm{RED}}}{2}$	Distinguish algal blooms from aquatic vegetation
Submerged Vegetation Sensitive Index (SVSI)	$\mathrm{SVSI} = \mathrm{TC1} - \mathrm{TC2}$	Distinguish submerged vegetation from water bodies

B_{NIR}, B_{RED}, B_{GREEN}, and B_{BLUE} represent the spectral reflectance of the corresponding bands; TC1 refers to the brightness component after the Tasseled Cap transformation; TC2 denotes the greenness component after the Tasseled Cap transformation.

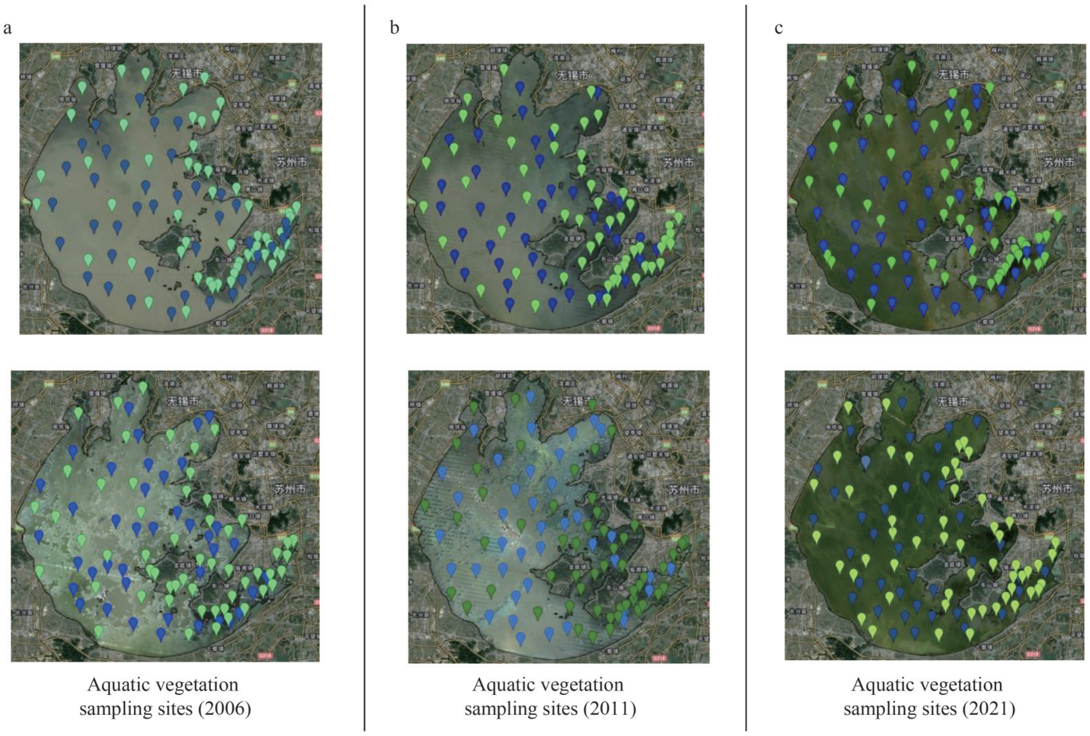

Fig.5 Spatial distribution of aquatic vegetation sampling sites in Taihu Lake during different years

a. sampling sites in 2006; b. sampling sites in 2011; c. sampling sites in 2021. Green areas represent aquatic vegetation, while blue areas represent non-aquatic vegetation.

Table 3 Confusion matrix for aquatic vegetation extraction in Taihu Lake

Season	Sensor type	Real/predicted class	Aquatic vegetation	Non-aquatic vegetation	Total real class samples
Summer	OLI	Aquatic vegetation	45(TP)	5(FN)	50
		Non-aquatic vegetation	3(FP)	42(TN)	45
		Total predicted class samples	48	47	95
	ETM+	Aquatic vegetation	45(TP)	5(FN)	50
		Non-aquatic vegetation	4(FP)	41(TN)	45
		Total predicted class samples	49	46	95
	TM	Aquatic vegetation	43(TP)	7(FN)	50
		Non-aquatic vegetation	5(FP)	40(TN)	45
		Total predicted class samples	48	47	95
Winter	OLI	Aquatic vegetation	44(TP)	6(FN)	50
		Non-aquatic vegetation	4(FP)	41(TN)	45
		Total predicted class samples	48	47	95
	ETM+	Aquatic vegetation	43(TP)	7(FN)	50
		Non-aquatic vegetation	4(FP)	41(TN)	45
		Total predicted class samples	47	48	95
	TM	Aquatic vegetation	42(TP)	8(FN)	50
		Non-aquatic vegetation	6(FP)	39(TN)	45
		Total predicted class samples	48	47	95

The $AVBPI_i$ represents the algal bloom frequency of individual pixels within the aquatic vegetation zone, reflecting the degree to which a vegetation pixel is repeatedly invaded by algal blooms. Specifically, $T_{cya\text{-}i}$ notes the number of valid observations during which the i^{th} vegetation pixel was identified as being affected by algal blooms within the target period, while $T_{val\text{-}i}$ represents the total number of valid observations for the i^{th} vegetation pixel during the same period (excluding invalid data such as clouds and shadows).

(2) The Vegetation Area Algal Bloom Proportion (VABP)

$$\mathrm{VABP} = \frac{N_{\mathrm{cya\text{-}veg}}}{N_{\mathrm{tot\text{-}veg}}} \times 100\%. \tag{2}$$

The VABP represents the proportion of algal bloom pixels within the aquatic vegetation area. Specifically, $N_{\mathrm{cya\text{-}veg}}$ denotes the total number of pixels identified as algal bloom within the aquatic vegetation zone during the target period, while $N_{\mathrm{tot\text{-}veg}}$ represents the total number of valid pixels within the vegetation zone.

AVBPI and VABP describe complementary aspects of algal bloom-vegetation interactions. AVBPI represents the long-term frequency of algal bloom occurrence within aquatic vegetation areas, reflecting the persistence and recurrence of bloom influence on vegetated habitats. VABP, in contrast, quantifies the relative spatial extent of bloom-affected pixels within vegetation areas at a given time, emphasizing instantaneous spatial overlap. Together, these indices distinguish repeated bloom intrusion from short-term areal overlap and provide an integrated view of bloom–vegetation interactions beyond simple bloom area metrics.

2.7 Encroachment channel identification

To reveal the spatial distribution characteristics and aggregation patterns of algal blooms in the study area, a spatial autocorrelation analysis was applied to systematically examine the spatial dependence of blooms at both the global and local scales. Areas with High-High (HH) clustering were identified as hotspots of frequent algal bloom occurrence and were regarded as potential primary encroachment channels.

At the global scale, the Moran's I index (Anselin, 1995) was used to evaluate the overall spatial correlation of algal blooms across the entire lake, determining whether their distribution pattern exhibited significant clustering, dispersion, or randomness. At the local scale, the Local Moran's I (LISA) method was employed to characterize the spatial clustering patterns and to further identify four typical types of spatial associations: HH clusters, Low-Low (LL) clusters, High-Low (HL) outliers, and Low-High (LH) outliers. This analysis reveals the internal spatial heterogeneity and hotspot distribution patterns of algal blooms within the lake.

The spatial weight matrix was constructed based on the adjacency relationships among lake grid cells, and the statistical significance of the clustering patterns was verified through significance testing. This approach effectively captures the spatial diffusion characteristics and dominant encroachment channels of algal blooms, providing essential spatial statistical support for subsequent water quality risk assessment, bloom monitoring, and prevention strategies.

2.8 Meteorological and environmental data

To investigate the regulatory effects of climate change and environmental variation on the interactions between algal blooms and aquatic vegetation, both meteorological and environmental monitoring datasets were integrated for analysis.

(1) Meteorological data: The meteorological indicators include precipitation and temperature, obtained from the 1-km-resolution monthly precipitation and temperature dataset of China (https://data.tpdc.ac.cn/). These data possess high spatial accuracy and temporal continuity, enabling effective characterization of the dynamic variations in climatic factors across the Taihu Basin.

(2) Environmental data: The environmental dataset includes key water quality parameters, namely total nitrogen (TN), total phosphorus (TP), chlorophyll *a* (Chl *a*), and the nitrogen-to-phosphorus ratio (TN/TP). These data were derived from the monthly water quality monitoring records (2005–2020) provided by the Taihu Lake Ecosystem Research Station, part of the Chinese Ecosystem Research Network (CERN).

Environmental variables (TN, TP, and Chl *a*) were analyzed only for the period with continuous in situ observations (2005–2020), while years with missing data (2003–2004 and 2021–2024) were excluded from environmental analyses to avoid uncertainties associated with data interpolation. As these missing years are limited to the beginning and the end of the study period, their exclusion does not affect the overall analysis of long-term patterns or the main conclusions of this study.

3 RESULT

3.1 Spatial distribution of algal blooms

The spatiotemporal distribution of algal bloom frequency from 2003 to 2024 is shown in Fig.6. Among the major bays of Taihu Lake, Zhushan Bay

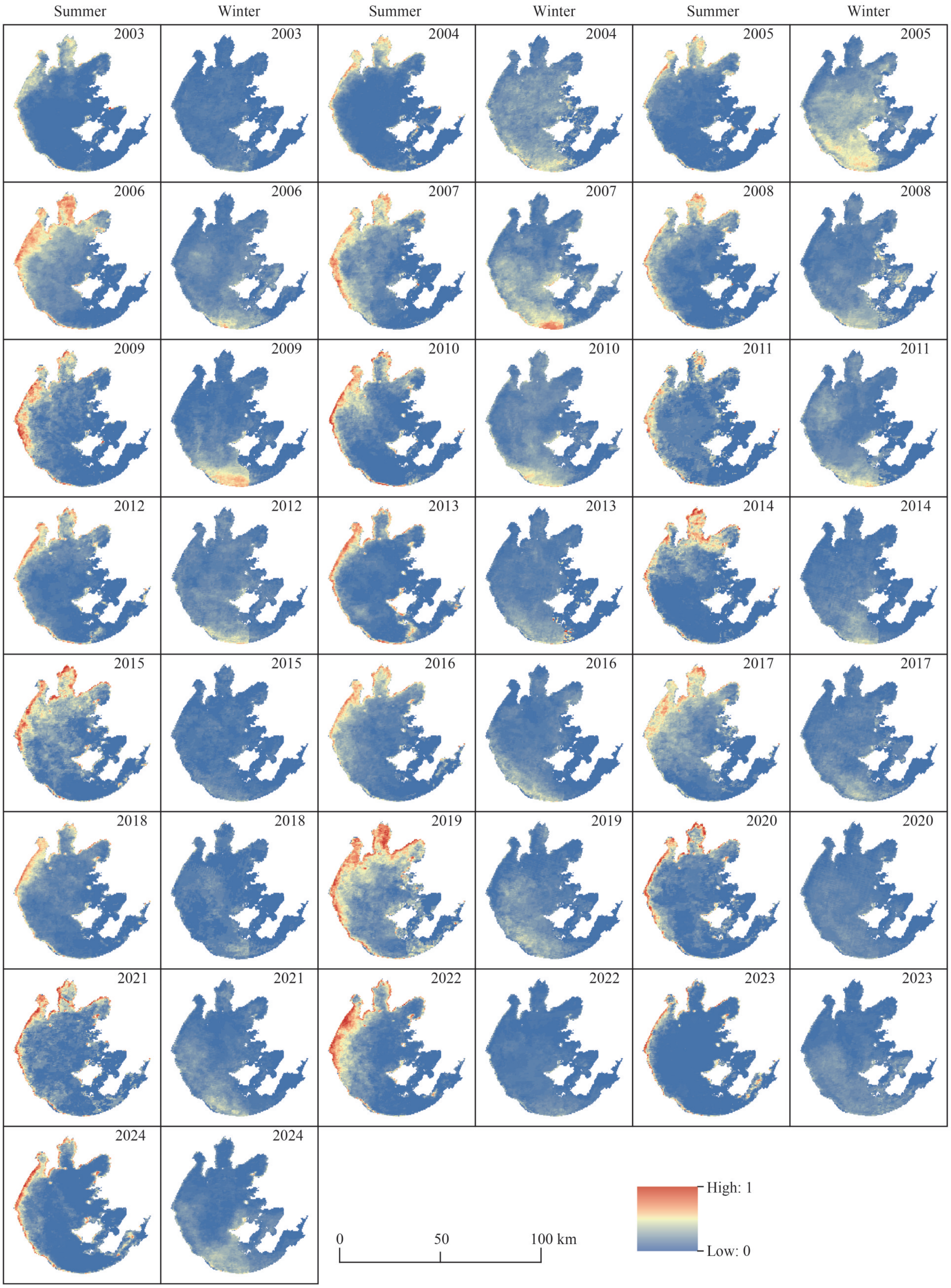

Fig.6 Spatiotemporal distribution of algal bloom frequency in Taihu Lake from 2003 to 2024 for summer and winter

The frequency of algal bloom occurrence is significantly higher in summer than in winter, with blooms showing a pronounced intrusion into Region 4 from the southern part of the lake.

exhibited the highest bloom frequency, followed by Meiliang Bay, while Gonghu Bay showed relatively lower occurrence probabilities. Seasonally, bloom frequency during summer was significantly higher than in winter, with the mean summer probability ranging between 5% and 20%, showing relatively minor interannual fluctuations.

Spatially, the eastern lake region displayed a much lower bloom frequency than the western region, and the probability of occurrence was consistently higher in summer than in winter. In summer, areas with high bloom frequency were mainly concentrated in Zones 1–4 of the eastern lake. Notably, in 2007, 2008, 2010, 2016, 2023, and 2024, several high-frequency patches emerged within the inner parts of the eastern lake, suggesting a gradual eastward expansion of algal blooms from the central basin.

In contrast, during winter, areas with relatively high bloom frequency were mostly located along the outer margins of the eastern lake, particularly in the southern part of Taihu Lake and around the southern coast of Xishan Island. These areas exhibited relatively high probabilities of bloom occurrence, whereas no obvious bloom signals were detected within the inner zones of the lake.

3.2 Validation and distribution of aquatic vegetation

The classification accuracy of aquatic vegetation extraction is summarized in Table 4. For all three Landsat sensors, the overall classification accuracy exceeded 80%, and the Kappa coefficients were higher than 0.7 (Pontius and Millones, 2011), indicating a high level of consistency between the classification results and the actual ground conditions. It is noteworthy that the classification accuracy exhibited a gradual improvement following the order TM<ETM+<OLI, confirming the superior signal-to-noise ratio and enhanced performance of the newer generation of sensors.

The spatial distribution of aquatic vegetation coverage in Taihu Lake from 2003 to 2024 during summer and winter is shown in Fig.7. Aquatic vegetation was mainly concentrated in Regions 2, 3, and 4, among which Region 4 had the largest vegetation-covered area, followed by Region 3, while Gonghu Bay exhibited the smallest coverage. Seasonally, the vegetation-covered area in summer was significantly larger than that in winter.

In terms of temporal variation, the summer vegetation area showed a declining-then-increasing trend over the study period. The coverage reached its lowest value in 2012, with only 177 km² of vegetation area recorded.

As shown in Fig.8a–b, before 2015, the summer aquatic vegetation area remained at a relatively high level, while the mean bloom frequency exhibited a significant upward trend, exceeding 10% in several years. In contrast, during winter, vegetation coverage declined markedly, yet the mean bloom frequency remained relatively high. After 2015, the summer aquatic vegetation area decreased sharply, accompanied by a sudden drop in mean bloom frequency. In the subsequent years, the vegetation area gradually recovered, and the bloom frequency began to rise again. Consistent with the summer trend, the winter vegetation area slightly and

Table 4 Accuracy assessment results of aquatic vegetation extraction in Taihu Lake

Season	Sensor type	Category	TP	FP	FN	TN	OA	UA	PA	Kappa coefficient
Summer	TM	Aquatic vegetation	43	5	7	40	0.873 7	0.895 8	0.860 0	0.747 2
		Non-aquatic vegetation	40	7	5	43	0.873 7	0.851 1	0.888 9	0.747 2
	ETM+	Aquatic vegetation	45	5	4	41	0.905 3	0.900 0	0.893 6	0.810 3
		Non-aquatic vegetation	41	4	5	45	0.905 3	0.911 1	0.918 4	0.810 3
	OLI	Aquatic vegetation	45	3	5	42	0.915 8	0.937 5	0.900 0	0.831 0
		Non-aquatic vegetation	42	5	3	45	0.915 8	0.893 6	0.933 3	0.831 0
Winter	TM	Aquatic vegetation	42	6	8	39	0.852 6	0.875 0	0.840 0	0.710 0
		Non-aquatic vegetation	39	8	6	42	0.852 6	0.829 8	0.866 7	0.710 0
	ETM+	Aquatic vegetation	43	4	7	41	0.884 2	0.914 9	0.860 0	0.768 4
		Non-aquatic vegetation	41	7	4	43	0.884 2	0.854 2	0.911 1	0.768 4
	OLI	Aquatic vegetation	44	4	6	41	0.894 7	0.916 7	0.880 0	0.789 0
		Non-aquatic vegetation	41	6	4	44	0.894 7	0.872 3	0.911 1	0.789 0

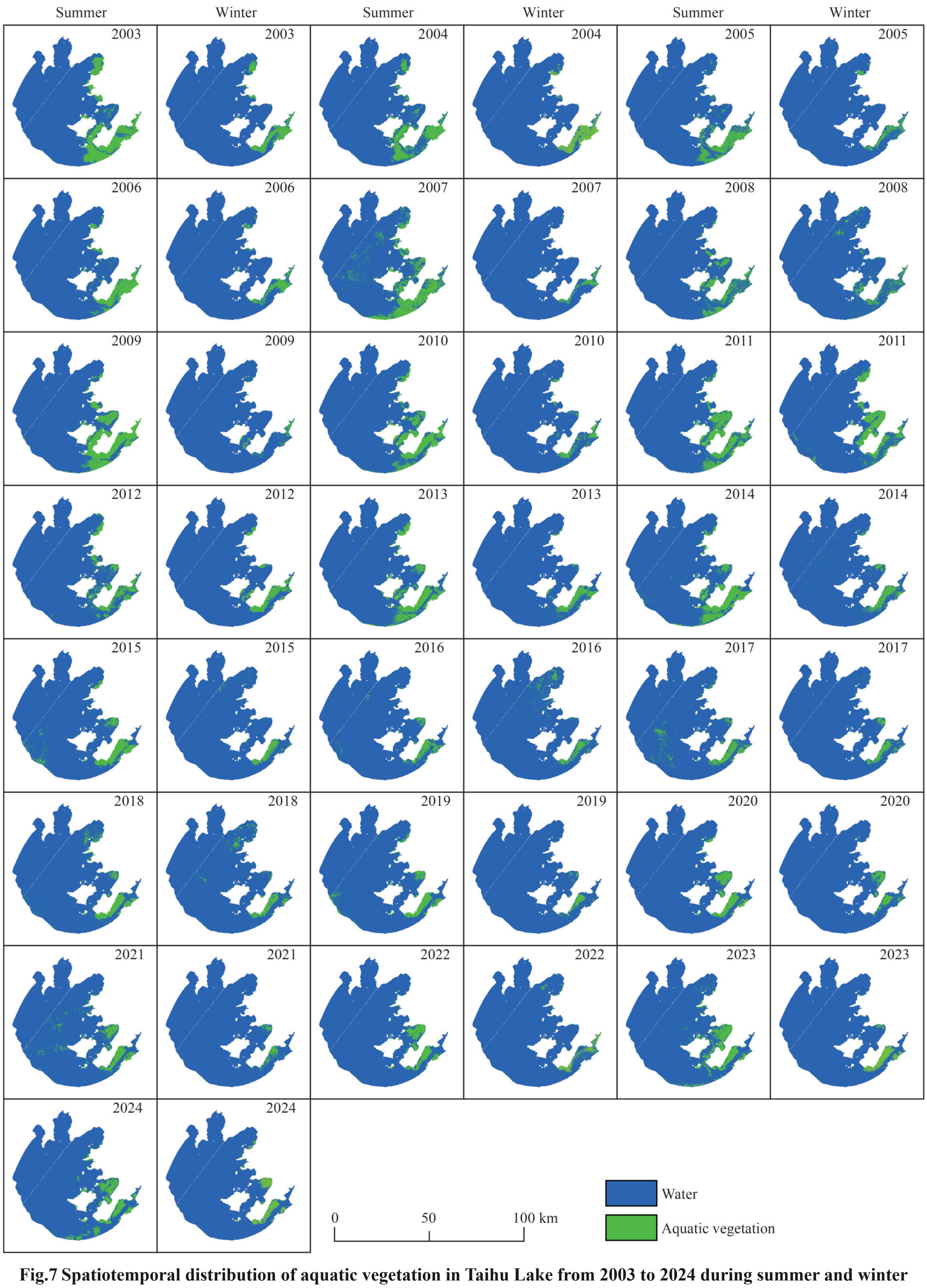

Fig.7 Spatiotemporal distribution of aquatic vegetation in Taihu Lake from 2003 to 2024 during summer and winter

Aquatic vegetation coverage is higher in summer than in winter, mainly distributed around Xishan Island in Region 3 and 4; in winter, the coverage decreases markedly and is primarily concentrated in Region 4.

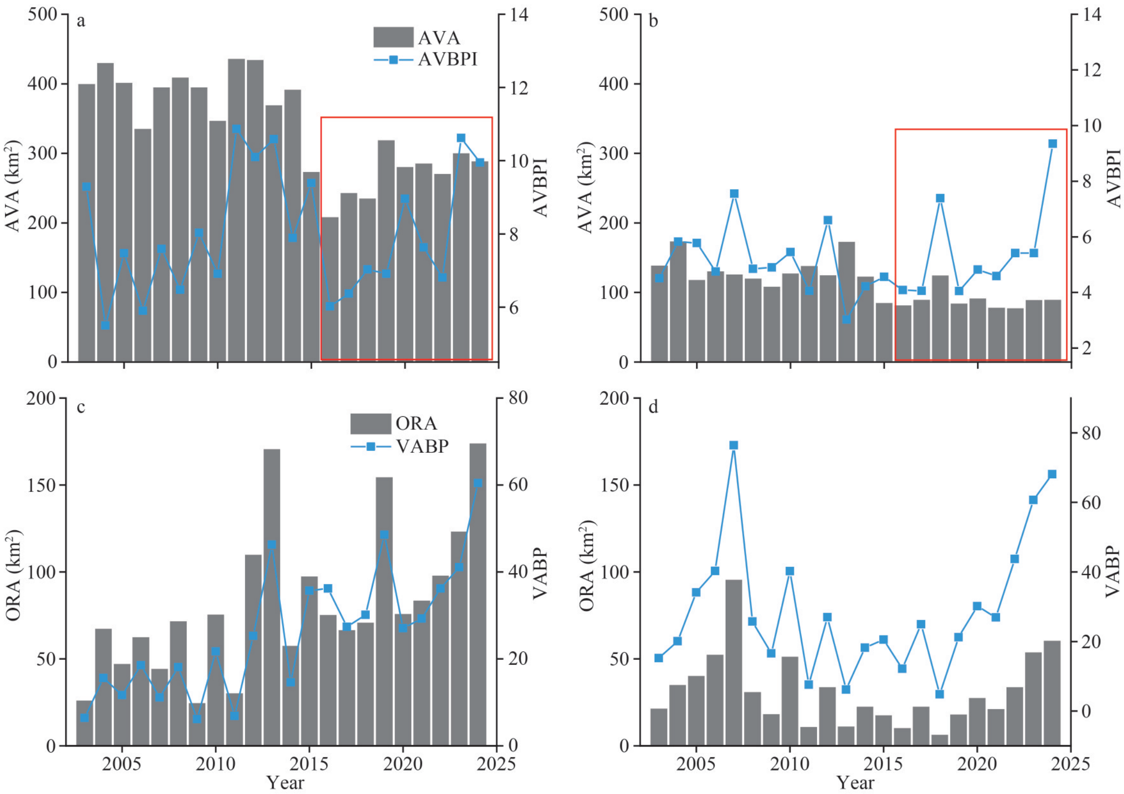

Fig.8 Trends of aquatic vegetation area and bloom occurrence in the eastern lake region

a. summer vegetation area (AVA) and AVBPI; b. winter vegetation area (AVA) and AVBPI; c. summer bloom-vegetation overlap area (ORA) and VABP; d. winter overlap area (ORA) and VABP. AVBPI (Algal Bloom Pixel Index in Vegetation Area) is a dimensionless frequency-based indicator representing the long-term recurrence of algal blooms within aquatic vegetation zones. VABP (Vegetation Area Algal Bloom Proportion) is a dimensionless proportion indicating the relative spatial extent of bloom-affected pixels within vegetation areas during a given period. AVBPI emphasizes repeated bloom intrusion, whereas VABP reflects instantaneous spatial overlap.

continuously declined around 2016, whereas the bloom frequency showed a persistent increase.

As illustrated in Fig.8c–d, both the summer bloom frequency and the overlap area between blooms and vegetation exhibited an increasing trend, indicating intensified bloom intrusion into vegetated regions. In contrast, the winter overlap dynamics appeared more complex; overall, the encroachment of algal blooms into vegetation areas intensified after 2015. Therefore, 2015 was selected as a critical turning point to divide the study period into two stages: Phase I (2003–2015), characterized by high vegetation coverage, and Phase II (2016–2024), when vegetation coverage declined substantially.

3.4 Encroachment channel of algal blooms

As shown in Fig.9, only HH clusters were retained to highlight areas with frequent occurrence and strong spatial aggregation of algal blooms. Overall, the spatial framework of algal bloom encroachment channels, inferred from long-term clustering patterns within aquatic vegetation zones in Taihu Lake, remains generally consistent across seasons and stages. However, clear differences emerge at both seasonal and stage scales, with the most pronounced variability occurring in Region 4.

Based on HH LISA clustering results, several statistically inferred encroachment channels were identified, representing spatial corridors of persistent high-frequency algal bloom aggregation rather than explicit transport pathways. In most cases, bloom expansion preferentially follows nearshore zones, forming shoreline-associated aggregation corridors. Channel 1, extending southward from Gonghu Bay, and Channel 2, surrounding Dongshan Island, represent two typical shoreline-hugging routes. Along these channels, bloom aggregation exhibits relatively weak seasonal and interannual variability, suggesting limited long-term buffering by aquatic vegetation. In contrast, bloom aggregation in Region 3 shows strong seasonal variability, with higher accumulation in winter, coinciding with reduced vegetation coverage

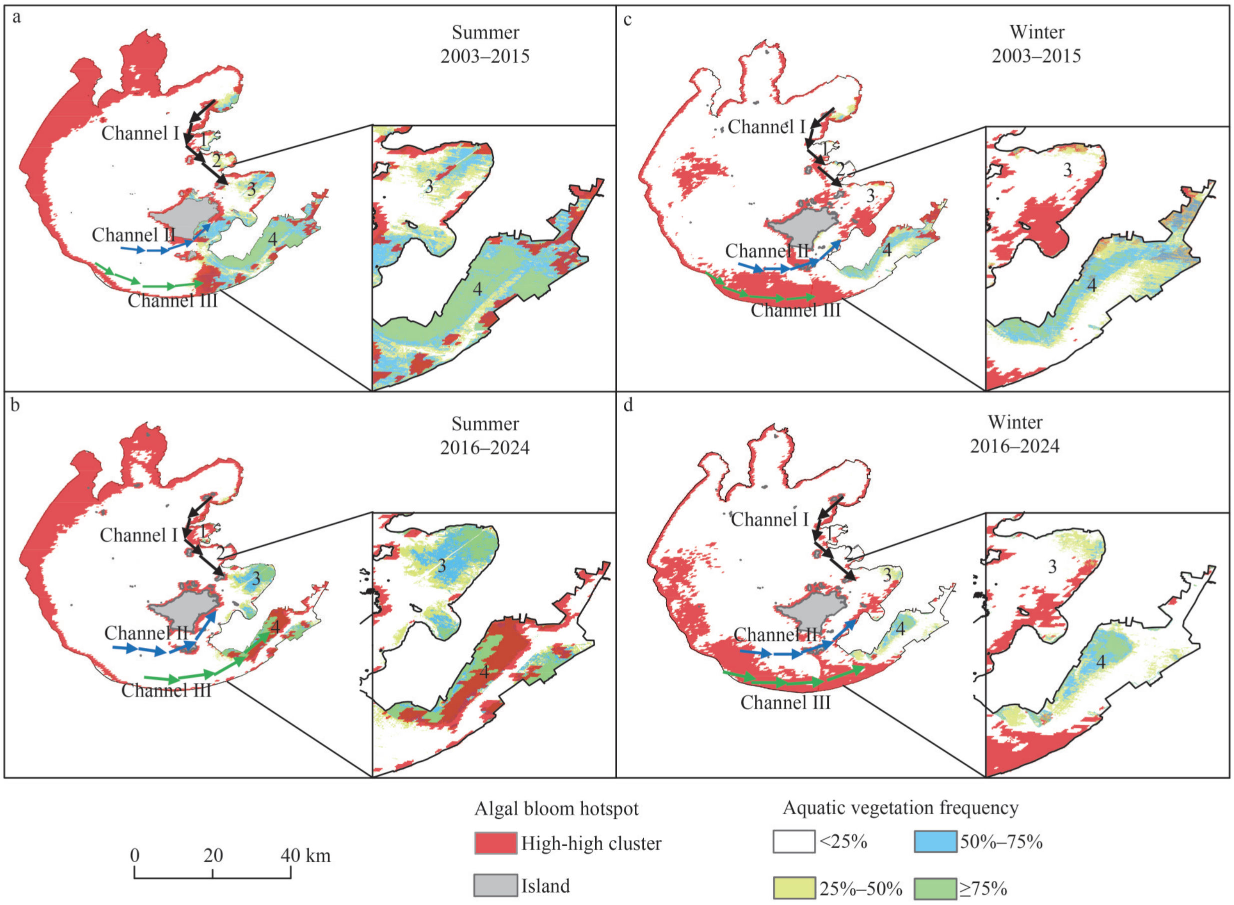

Fig.9 Statistically inferred encroachment channels of algal blooms in Taihu Lake derived from HH LISA clusters, representing persistent spatial aggregation corridors rather than physical transport routes

a. summer, Phase I (2003–2015); b. summer, Phase II (2016–2024); c. winter, Phase I (2003–2015); d. winter, Phase II (2016–2024). Channel I extends southward along the shoreline of Gonghu Bay, Channel II surrounds Dongshan Island, and Channel III affects the southern lake margin.

and enhanced bloom presence across open-water areas toward Regions 3 and 4.

Seasonal contrasts between summer and winter reveal marked differences in bloom aggregation intensity and spatial extent. During summer, bloom hotspots display stronger aggregation and broader spatial coverage, particularly in the eastern interior of Region 4, indicating enhanced internal bloom development and accumulation within this region. In winter, bloom hotspots become more fragmented, and high-value aggregation areas within Region 4 are substantially reduced, while seasonal differences in Regions 1–3 remain relatively limited.

Stage-based comparisons between Phase I (2003–2015) and Phase II (2016–2024) further highlight Region 4 as the primary area of change. During Phase I, bloom clusters in Region 4 are spatially limited and weakly connected. In contrast, during Phase II, both aggregation intensity and spatial connectivity increase markedly, particularly in the eastern part of the region. Spatial patterns in Regions 1–3, however, remain largely stable between the two stages.

In summary, although the large-scale spatial configuration of encroachment channels in Taihu Lake remains relatively stable, bloom aggregation within Region 4—especially in its eastern interior—emerges as the dominant contributor to seasonal and stage-dependent variability. This enhancement becomes more pronounced following substantial aquatic vegetation degradation, indicating a weakening of the long-term buffering function of vegetation against bloom expansion.

4 DISCUSSION

4.1 Evaluation of aquatic vegetation and algal bloom extraction results

4.1.1 Spatiotemporal distribution of algal blooms

From 2003 to 2024, high-frequency algal bloom occurrence in Taihu Lake consistently concentrated in Meiliang Bay (northern lake), Zhushan Bay, Gonghu Bay, and along the western shoreline, a spatial pattern consistent with previous long-term remote-sensing reconstructions (Duan et al., 2009). Existing studies generally attribute the frequent blooms in nearshore areas to strong terrestrial nutrient inputs and relatively enclosed bay geomorphology, which together lead to elevated TN and TP concentrations and favor persistent bloom occurrence (Jin et al., 2015). In this context, the spatiotemporal variability of TP has been widely recognized as an effective indicator of eutrophication status and bloom risk (Xiong et al., 2022). Building on these findings, our results further indicate that under non-extreme bloom conditions, algal blooms and aquatic vegetation can coexist over certain time scales without exhibiting a strictly unidirectional suppressive or facilitative relationship, consistent with observations reported by Breininger et al. (2017).

Compared with previous long-term remote-sensing studies of algal blooms in Taihu Lake, the present study differs markedly in research perspective and spatial characterization. Duan et al. (2009), Shi et al. (2015), and Jia et al. (2019) primarily reconstructed long-term temporal variations in bloom area, frequency, or intensity and examined their responses to meteorological factors and nutrient conditions; however, bloom expansion was generally treated as an area-based process, without explicitly resolving propagation directions or internal spatial organization within the lake. By contrast, our multi-year analysis reveals that algal blooms in Taihu Lake do not expand isotropically. Instead, bloom expansion follows a progressive west-to-east pattern (Duan et al., 2009; Chen et al., 2020) , forming relatively stable and directional expansion corridors along the northern and southern margins of Xishan Island and in the southern lake area, linking algal-dominated source regions with aquatic vegetation-dominated recipient zones.

Previous studies have shown that the duration, redistribution, and re-aggregation of cyanobacterial blooms at short time scales in Taihu Lake are primarily controlled by meteorological forcing and hydrodynamic processes. For example, Min et al. (2019) and Chen et al. (2020) demonstrated that under the combined effects of wind-driven circulation and bay geomorphology, blooms tend to undergo directional redistribution along nearshore and semi-enclosed embayments, generally expanding from the western and northern bays toward the eastern lake. In addition, Huang et al. (2025) integrated machine learning techniques with GOCI data to achieve short-term spatial prediction of algal blooms in Taihu Lake, revealing that wind speed, air temperature, and antecedent algal biomass are the key drivers governing bloom formation and dispersal processes. Xue et al. (2023) and Zhu et al. (2014) reported that strong wind or storm events can further enhance repeated bloom accumulation in specific shoreline zones, thereby intensifying spatial heterogeneity. Against this background, the HH LISA-identified bloom hotspots in this study indicate that bloom expansion exhibits a stable, channelized spatial structure in a long-term statistical sense. Such spatial configurations are broadly consistent with long-term bloom accumulation zones documented by hydrodynamic and wind-driven analyses in Taihu Lake (Zhu et al., 2014; Min et al., 2019; Chen et al., 2020), as well as by multi-year remote-sensing observations revealing persistent bloom concentration patterns (Duan et al., 2009; Shi et al., 2015). It should be emphasized that the encroachment channels identified here do not represent explicit bloom transport directions or movement processes. Instead, they reflect statistically inferred spatial organization patterns emerging from recurrent high-frequency bloom occurrence over multi-year periods. As discussed by Jin et al. (2015), long-term nutrient redistribution can shape persistent bloom-prone regions, while studies by Paerl and Otten (2013) and Hilt et al. (2018) highlight that the weakening buffering capacity of aquatic vegetation and broader ecological structural adjustments jointly contribute to the stabilization of such large-scale spatial patterns in eutrophic shallow lakes.

4.1.2 Distribution of aquatic vegetation

The results of this study show that aquatic vegetation in Taihu Lake was primarily distributed in Regions 2, 3, and 4, with the largest vegetation coverage observed in Region 4, followed by Region 3 and Region 2. Using a similar decision tree classification approach, Yang et al. (2021) extracted aquatic vegetation in East Taihu Lake from 2017 to 2019, and their findings are largely consistent with those of the present study. In 2017, vegetation coverage in East Taihu Lake exhibited no significant seasonal differences between summer and winter, whereas in 2019, vegetation in Region 4 decreased markedly. The spatial distribution patterns of aquatic vegetation derived by Luo et al. (2023) also agree well with our results, indicating the high reliability of the identification method employed in this study.

Notably, a substantial reduction in aquatic vegetation occurred during 2015–2016, primarily in Region 3, which is likely associated with a combination of natural and anthropogenic pressures, considered here as plausible contributing factors rather than quantitatively confirmed drivers. First, intensified eutrophication and frequent algal blooms substantially reduced water transparency, limiting underwater light availability and continuously suppressing the recovery of aquatic vegetation (Zhao et al., 2017). In parallel, human disturbances such as dredging, shoreline modification, and fishery activities degraded local habitat conditions (Zhao et al., 2015). National-level policy documents further indicate that during 2015–2016, East Taihu Lake and its surrounding areas were subject to sustained large-scale remediation and engineering interventions, including lake embankment reinforcement (34.93 km of embankments with 30 sluice control structures and the construction or reconstruction of harbors), flood conveyance channel construction (12.2 km in length with a bottom width of 200 m), and comprehensive regulation of inflow and outflow channels (19 channels totaling 29.63 km, including 22.48 km of dredging and 7.14 km of bank restoration with a fish passage) (Ministry of Ecology and Environment of the People's Republic of China, 2016). This engineering context provides a plausible anthropogenic background for the reduction of aquatic vegetation in eastern Taihu Lake during 2015–2016. Meanwhile, shifts in community composition, marked by the retreat of submerged macrophytes and the expansion of floating-leaved and emergent species, likely further amplified vegetation loss (Zhang et al., 2018). Taken together, the pronounced decline of aquatic vegetation in Region 3 in 2016 is best interpreted as the combined outcome of deteriorating water quality and intensified human disturbance. Moreover, this abrupt vegetation decline during 2015–2016 also coincides with a reorganization of algal bloom aggregation patterns identified in this study. Following vegetation loss, bloom aggregation intensified and expanded into vegetation-dominated regions along specific encroachment channels, particularly in Region 4. This suggests that years with rapid vegetation degradation represent critical transition points in bloom-vegetation interactions, during which encroachment channels become more active and spatially pronounced. This further supports the view that encroachment channel dynamics provide a sensitive spatial indicator of regime shifts in bloom-vegetation interactions.

4.2 Relationship between algal blooms and aquatic vegetation

Figure 10a–b illustrates the correlations between aquatic vegetation indicators and major environmental variables during summer and winter, while Fig.10c–d further isolates the relatively independent effects of these relationships using partial correlation analysis. Overall, environmental controls on aquatic vegetation coverage and algal bloom encroachment are more pronounced in summer and weaken substantially in winter, indicating a strong seasonal dependence of bloom intrusion into vegetated areas (Qin et al., 2010).

In summer, Chl *a* shows a significant negative correlation with AVA, indicating that the expansion of algal blooms into aquatic vegetation zones constrains vegetation coverage. This pattern is consistent with bloom-induced light limitation and habitat degradation commonly observed in shallow lakes. Meanwhile, AVA is significantly positively correlated with the TN/TP ratio and negatively correlated with VABP, suggesting that algal blooms are more likely to intrude into vegetated areas under lower TN/TP conditions. Because reduced TN/TP ratios generally reflect more severe eutrophication, this result implies enhanced competitive dominance of algae under such conditions (Conley et al., 2009; Naderian et al., 2025). Partial correlation analysis further identifies Chl *a*, Temp., and TN as important factors influencing aquatic vegetation dynamics in summer. After controlling for other environmental variables, the persistently significant negative relationship between Chl *a* and AVA indicates a relatively independent suppressive effect of intensified blooms on vegetation expansion through reduced water transparency and habitat alteration, a mechanism widely documented in eutrophic shallow lakes (Scheffer et al., 1993, 2001; Paerl and Otten, 2013; Hilt et al., 2018). In addition, the significant negative association between Temp. and AVA suggests that warming may further enhance the competitive advantage of algal blooms over aquatic vegetation (Paerl and Otten, 2013; Hilt et al., 2018;). In contrast, TN/TP shows generally weak correlations with most vegetation and encroachment indicators, indicating that nutrient stoichiometry is

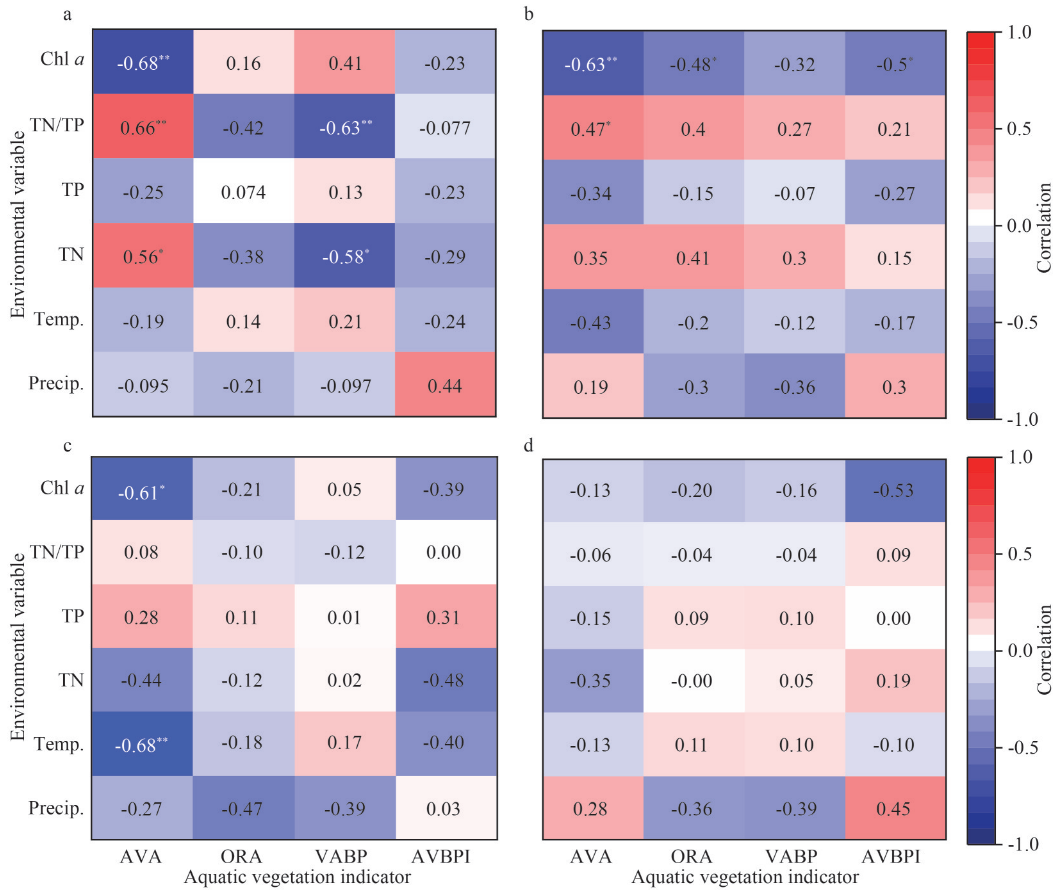

Fig.10 Correlation and detrended partial correlation heatmaps between aquatic vegetation indicators (AVA, ORA, VABP, and AVBPI) and environmental variables in Taihu Lake during summer and winter

a. Pearson correlation coefficients in summer; b. Pearson correlation coefficients in winter; c. correlation and detrended partial correlation heatmaps between aquatic vegetation indicators (AVA, ORA, VABP, and AVBPI) and environmental variables in summer; d. correlation and detrended partial correlation heatmaps between aquatic vegetation indicators (AVA, ORA, VABP, and AVBPI) and environmental variables in winter. Temp.: temperature; precip.: precipitation; AVA: aquatic vegetation area; ORA: overlap area; VABP: vegetation-area bloom pixel ratio. *: $P<0.05$ indicates significance; **: $P<0.01$ indicates high significance.

unlikely to act as a single direct driver of encroachment structure, but rather serves as an integrated indicator of background nutrient conditions and competitive regimes (Reynolds, 2006; Paerl and Otten, 2013; Hilt et al., 2018).

In winter, overall bloom intensity decreases, and correlations between environmental variables and aquatic vegetation indicators are generally weaker. Nevertheless, Chl *a* remains significantly negatively correlated with AVA, indicating that algal blooms continue to exert competitive pressure on aquatic vegetation even under reduced bloom intensity. Significant negative associations between Chl *a* and ORA as well as VABP likely reflect suppressed phytoplankton physiological activity under low temperatures and enhanced hydrodynamic disturbance that limits sustained bloom aggregation, a pattern previously reported for Taihu Lake and other shallow lakes (Zhu et al., 2014). Partial correlation results further show that relationships between environmental factors and vegetation or encroachment indicators are overall weakened in winter, indicating that thermal constraints and hydrodynamic processes dominate during the non-growing season (Zhu et al., 2014; Wu et al., 2015).

It should be noted that, compared with simple correlation analysis, partial correlation analysis alters the significance of some variables after controlling for covariates. Specifically, after controlling for TN/TP, the correlations between TN and several vegetation or encroachment indicators become insignificant; conversely, when both TN and TP are controlled for, the statistical significance of TN/TP is also markedly reduced. This pattern indicates that TN and TN/TP exhibit a certain degree of statistical covariance, and their effects are more strongly expressed at the level of integrated nutrient background conditions rather than as independent driving factors (Reynolds, 2006; Paerl and Otten, 2013; Hilt et al., 2018). These results further support the interpretation that nutrient stoichiometry in this study primarily reflects background nutrient status and competitive environments, rather than acting as a single controlling factor directly determining algal bloom encroachment structure (Zhang et al., 2016).

4.3 Application and policy implications

Taihu Lake is a unique shallow-lake system characterized by the long-term coexistence of extensive algal blooms and densely vegetated eastern bays under intensive human intervention and ecological management. Unlike many eutrophic lakes where blooms are mainly confined to open-water regions, algal blooms in Taihu frequently interact with nearshore aquatic vegetation and water-intake zones, making bloom transport channels and vegetation buffering capacity central issues for lake governance and drinking-water security.

Long-term intake-based risk assessment indicates that algal blooms in Taihu Lake have progressively expanded from traditional source areas in the northern and western lake toward the eastern lake and intake zones under the combined influence of wind-driven circulation and lake hydrodynamics. Figure 11 shows the locations of the various water intakes of Taihu Lake, with a 3-km buffer zone for each intake. It can be seen that from 2003 to 2024, bloom probability within 3-km intake buffer zones shows a fluctuating but overall increasing trend, particularly during high-temperature seasons, suggesting a sustained pressure on drinking-water safety despite recent nutrient-reduction and diversion measures.

Marked spatial heterogeneity is observed among intake sites. The Gonghu Bay intakes (intake_a, b, c) are consistently exposed to the highest bloom risk, as they are located along persistent bloom transport channels linking Meiliang Bay and Zhushan Bay with the eastern lake. Dominant wind fields and nearshore retention further promote bloom accumulation in this area. In contrast, central and southern intakes (intake_d, e, f, g) exhibit lower bloom probability, which is associated with stronger water exchange, higher transparency, and more stable aquatic vegetation conditions.

These results support region-specific bloom management strategies in Taihu Lake. The Gonghu Bay intake zone should be prioritized for targeted interventions, such as maintaining or restoring nearshore aquatic vegetation, establishing ecological buffer belts, or deploying temporary bloom-blocking facilities during high-risk periods. For central and southern intake areas, maintaining existing hydrodynamic conditions and vegetation

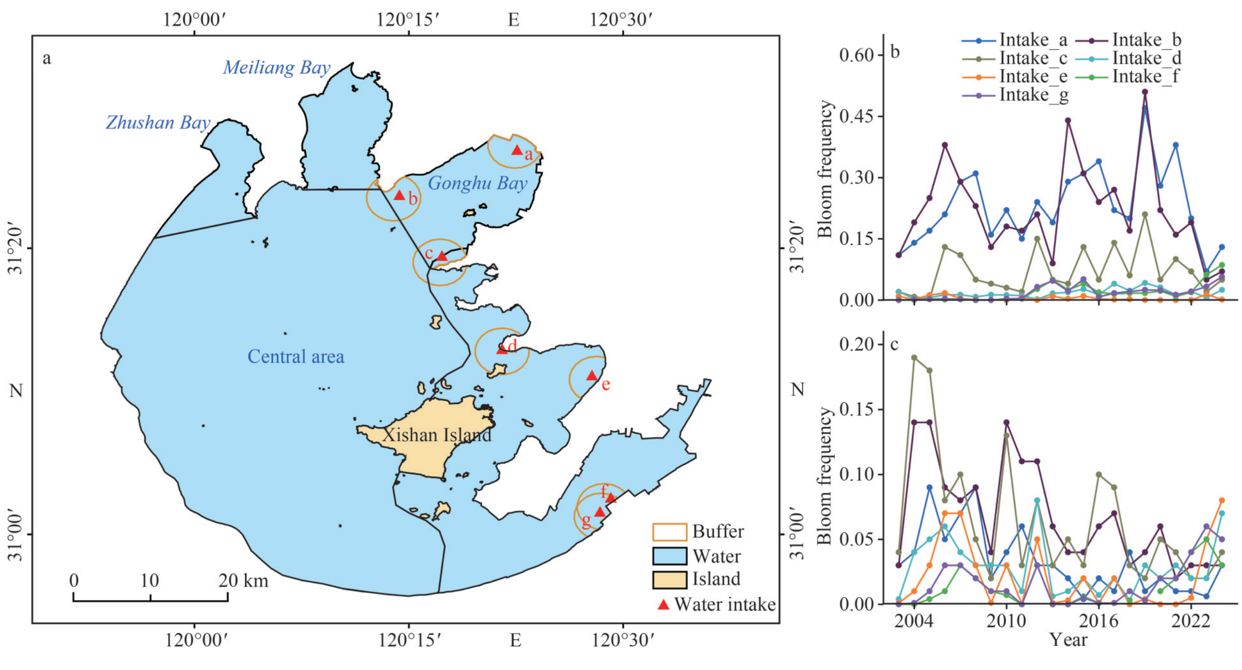

Fig.11 Bloom risk assessment at water-intake locations

a. the 3-km buffer zone of all water intakes; b. summer bloom frequency at each intake; c. winter bloom frequency at each intake.

structure is essential to prevent system degradation. In addition, the increasing likelihood of locally generated blooms in Region 4 highlights the need for enhanced monitoring and source identification to support adaptive management and early warning.

4.4 Limitation

4.4.1 Algorithm applicability and robustness

It should be noted that the bloom and aquatic vegetation identification algorithms adopted in this study are not newly developed, but have been extensively applied and validated in numerous previous studies in Taihu Lake and other large shallow lakes with complex optical conditions. In this study, algal blooms were identified using a decision tree classification approach that integrates the FAI, TWI, and CMI. This method has been widely applied to detect algal blooms in optically complex waters (Hu, 2009; Feng et al., 2012; Liang et al., 2017) and has become a methodological foundation for reconstructing long-term algal bloom dynamics in Taihu Lake using MODIS observations (Duan et al., 2009). Similarly, for Taihu Lake—a shallow lake characterized by complex optical conditions—numerous long-term studies have developed and validated satellite-based aquatic vegetation retrieval methods based on vegetation indices specifically adapted to such environments, and these techniques are now considered mature and reliable in this region (Shi et al., 2015; Yang et al., 2021).

In the present study, these well-established algorithms were applied in a consistent and conservative manner, with an emphasis on long-term and relative spatial patterns rather than on single-date absolute area estimates. By independently retrieving algal blooms and aquatic vegetation using literature-supported indices and threshold settings, potential cross-interference between the two targets under bloom-vegetation coexistence conditions was minimized. The persistence of identified encroachment channels and hotspot patterns across different seasons and stages further indicates that the main conclusions of this study are not sensitive to minor algorithmic uncertainties, but instead reflect robust large-scale and long-term spatial organization.

4.4.2 Other methodological limitation

Several limitations of this study should be acknowledged. First, the identification of algal blooms and aquatic vegetation was based on threshold-driven remote sensing indices and decision-tree classification schemes. Although these methods have been widely validated and applied in previous studies, uncertainties associated with threshold selection, sensor-specific spectral responses, and atmospheric conditions cannot be completely eliminated. Such uncertainties may affect pixel-level classification accuracy but are unlikely to substantially alter the long-term, regional-scale spatiotemporal patterns emphasized in this study.

Second, uncertainties inherent to satellite remote sensing, including mixed-pixel effects, cloud contamination, and spatial resolution limitations, may influence the precision of bloom and vegetation boundaries, particularly in nearshore and transition zones. However, the encroachment-related indicators used here (e.g., AVBPI and VABP) are based on pixel-frequency and proportion statistics, which are more robust to boundary uncertainty than exact geometric area estimates and are therefore suitable for characterizing long-term encroachment intensity.

Third, this study integrates multi-source satellite datasets with different spatial resolutions. While algal blooms and aquatic vegetation were extracted independently from MODIS and Landsat data, respectively, potential scale effects cannot be entirely avoided. Nevertheless, our analyses focus on relative spatial organization, hotspot patterns, and long-term variability, rather than fine-scale spatial correspondence, thereby reducing the influence of resolution mismatch on the main conclusions.

In addition, remote sensing methods cannot effectively distinguish phytoplankton species, and algal blooms may be spectrally mixed with floating-leaved vegetation. In this study, floating-leaved vegetation was not explicitly separated during bloom identification; however, ts limited spatial extent in Taihu Lake (approximately 6% of the total lake area; Zhao et al., 2013) suggests that the resulting uncertainty is acceptable for long-term analyses. Therefore, species-specific or functional-type-specific responses cannot be fully resolved in this study. However, as this study focuses on relative spatial patterns, frequency-based indicators, and long-term encroachment channels rather than absolute bloom area estimates, the persistence of major hotspot patterns and encroachment corridors across seasons and stages suggests that the main conclusions are robust to moderate threshold-related uncertainties.

Furthermore, although wind-driven transport and the vertical migration of buoyant cyanobacteria (e.g., *Microcystis*) are known to play important roles in short-term bloom movement and accumulation, these processes were not explicitly incorporated into the present analysis. This is because the primary focus of this study is on seasonal to interannual patterns and long-term encroachment channels derived from multi-year satellite observations, at which scale the effects of short-term meteorological events and diel vertical migration are largely integrated into frequency-based metrics. Moreover, the encroachment channels identified in this study are inferred from long-term spatial clustering patterns of algal blooms and have not been independently validated against hydrodynamic circulation models, wind field simulations, or in situ transport observations.

Finally, the relationships between environmental factors, algal blooms, and aquatic vegetation identified in this study are primarily based on statistical associations. While these results provide important insights into potential regulatory mechanisms, they do not establish direct causality. Future studies combining high-frequency meteorological observations, hydrodynamic modeling, and in situ experiments would help further elucidate the mechanistic processes governing bloom encroachment and vegetation dynamics.

5 CONCLUSION

Taihu Lake is a highly eutrophic shallow lake characterized by the long-term coexistence of frequent algal blooms in the western lake and extensive aquatic vegetation in the eastern bays. Based on 22 years of multi-source remote sensing observations, this study systematically characterized the spatiotemporal dynamics of algal blooms and aquatic vegetation and identified persistent encroachment channels linking bloom source regions with vegetated zones.

Algal blooms were consistently concentrated in Meiliang Bay, Zhushan Bay, Gonghu Bay, and the western shoreline, exhibiting an overall increasing occurrence trend. Aquatic vegetation was mainly distributed in the eastern bays and remained relatively stable prior to 2015, followed by a sharp decline around 2016 and subsequent recovery. Long-term analyses reveal a generally negative association between algal blooms and aquatic vegetation, modulated by seasonal climate conditions and nutrient status.

Spatial autocorrelation analysis further demonstrates that bloom expansion is not spatially homogeneous but follows several persistent channels, particularly along the northern shoreline of Gonghu Bay, around Dongshan Island, and along the southern lake margin. Vegetation degradation, especially in Region 4 after 2015, coincided with enhanced bloom aggregation and increased susceptibility to locally generated blooms, indicating a weakening of the ecological buffering function.

From a management perspective, aquatic vegetation plays a critical role in mitigating bloom intrusion and protecting drinking-water security. Gonghu Bay intake areas represent priority zones for bloom prevention due to their exposure to dominant transport channels, whereas maintaining vegetation structure and hydrodynamic conditions is essential for reducing bloom risk in central and southern intake regions. Overall, the channel-based framework developed in this study provides a useful spatial perspective for understanding long-term bloom-vegetation interactions and supports region-specific strategies for bloom control and ecological restoration in Taihu Lake.

6 DATA AVAILABILITY STATEMENT

The remote sensing datasets used in this study are publicly available. MOD09GA surface reflectance data and Landsat 5 TM, Landsat 7 ETM+, and Landsat 8 OLI Level-2 surface reflectance datasets can be accessed from the official data providers and were processed in Google Earth Engine. The derived datasets generated during the current study are available from the corresponding author on reasonable request.

References

Anselin L. 1995. Local indicators of spatial association—LISA. *Geographical Analysis*, **27**(2): 93-115, https://doi.org/10.1111/j.1538-4632.1995.tb00338.x.

Bilous O P, Nezbrytska I, Zhezherya V et al. 2023. Interactions between aquatic plants and cyanobacterial blooms in freshwater reservoir ecosystems. *Water*, **15**(4): 672, https://doi.org/10.3390/w15040672.

Breininger D R, Breininger R D, Hall C R. 2017. Effects of surrounding land use and water depth on seagrass dynamics relative to a catastrophic algal bloom. *Conservation Biology*, **31**(1): 67-75, https://doi.org/10.1111/cobi.12791.

Chen H M, Zhu Y Y, Zhang Y et al. 2020. Cyanobacterial bloom expansion caused by typhoon disturbance in Lake Taihu China. *Environmental Science and Pollution Research*, **27**(34): 42294-42303, https://doi.org/10.1007/s11356-020-09292-0.

Conley D J, Paerl H W, Howarth R W et al. 2009. Controlling Eutrophication: nitrogen and phosphorus. *Science*, **323**(5917): 1014-1015, https://doi.org/10.1126/science.1167755.

Duan H T, Ma R H, Xu X F et al. 2009. Two-decade reconstruction of algal blooms in China's Lake Taihu. *Environmental Science & Technology*, **43**(10): 3522-3528, https://doi.org/10.1021/es8031852.

Feng L, Hu C M, Chen X L et al. 2012. Human induced turbidity changes in Poyang Lake between 2000 and 2010: observations from MODIS. *Journal of Geophysical Research*: *Oceans*, **117**(C7): C07006, https://doi.org/10.1029/2011JC007864.

Foody G M. 2002. Status of land cover classification accuracy assessment. *Remote Sensing of Environment*, **80**(1): 185-201, https://doi.org/10.1016/S0034-4257(01)00295-4.

Hilt S, Alirangues Nuñez M M, Bakker E S et al. 2018. Response of submerged macrophyte communities to external and internal restoration measures in north temperate shallow lakes. *Frontiers in Plant Science*, **9**: 194, https://doi.org/10.3389/fpls.2018.00194.

Hu C M. 2009. A novel ocean color index to detect floating algae in the global oceans. *Remote Sensing of Environment*, **113**(10): 2118-2129, https://doi.org/10.1016/j.rse.2009.05.012.

Hu C M, Lee Z, Ma R H et al. 2010. Moderate resolution imaging spectroradiometer (MODIS) observations of cyanobacteria blooms in Taihu Lake, China. *Journal of Geophysical Research*: *Oceans*, **115**(C4): C04002, https://doi.org/10.1029/2009JC005511.

Huang Z H, Ma R H, Liu H Z et al. 2025. Short-term spatial prediction of algal blooms in Lake Taihu Via machine learning and GOCI observations. *Journal of Environmental Management*, **388**: 125964, https://doi.org/10.1016/j.jenvman.2025.125964.

Iacarella J C, Barrow J L, Giani A et al. 2018. Shifts in algal dominance in freshwater experimental ponds across differing levels of macrophytes and nutrients. *Ecosphere*, **9**(1): e02086, https://doi.org/10.1002/ecs2.2086.

Jin Y W, Zhu G W, Xu H et al. 2015. Spatial distribution pattern and stock estimation of nutrients during bloom season in Lake Taihu. *Environmental Science*, **36**(3): 936-945. (in Chinese with English abstract)

Lei Z X. 2006. Study on Aquatic Macrophyte Vegetations and Their Environment Effects in Taihu Lake. Ji'nan University, Guangzhou. (in Chinese)

Li D H, Li G B, Chen W X et al. 2009. Interactions between a cyanobacterial bloom (*Microcystis*) and the submerged aquatic plant *Ceratophyllum oryzetorum* Kom. *Chinese Journal of Oceanology and Limnology*, **27**(1): 38-42, https://doi.org/10.1007/s00343-009-0038-7.

Liang Q C, Zhang Y C, Ma R H et al. 2017. A MODIS-based novel method to distinguish surface cyanobacterial scums and aquatic macrophytes in Lake Taihu. *Remote Sensing*, **9**(2): 133, https://doi.org/10.3390/rs9020133.

Liu X Y, Sun T, Yang W et al. 2024. Meta-analysis to identify inhibition mechanisms for the effects of submerged plants on algae. *Journal of Environmental Management*, **355**: 120480, https://doi.org/10.1016/j.jenvman.2024.120480.

Luo J H, Ma R H, Duan H T et al. 2014. A new method for modifying thresholds in the classification of tree models for mapping aquatic vegetation in Taihu Lake with Satellite Images. *Remote Sensing*, **6**(8): 7442-7462, https://doi.org/10.3390/rs6087442.

Luo J H, Ni G G, Zhang Y L et al. 2023. A new technique for quantifying algal bloom, floating/emergent and submerged vegetation in eutrophic shallow lakes using Landsat imagery. *Remote Sensing of Environment*, **287**: 113480, https://doi.org/10.1016/j.rse.2023.113480.

Markham B, Storey J, Morfitt R. 2015. Landsat-8 sensor characterization and calibration. *Remote Sensing*, **7**(3): 2279-2282, https://doi.org/10.3390/rs70302279.

Min Z, Zhen Y, Xiaoli S. 2019. Expansion and drivers of cyanobacterial blooms in Lake Taihu. *Journal of Lake Sciences*, **31**(2): 336-344. https://doi.org/10.18307/2019.0203.

Ministry of Environmental Protection of the People's Republic of China. 2016. Approval of the environmental impact report for the follow-up works of the East Taihu comprehensive improvement project. Ministry of Environmental Protection of the People's Republic of China. Huan Shen [2016] No. 64. https://www.mee.gov.cn/gkml/sthjbgw/spwj1/201605/t20160513_337630.htm. Accessed on 2016-05-11.

Naderian D, Noori R, Kim D et al. 2025. Environmental controls on the conversion of nutrients to chlorophyll in lakes. *Water Research*, **274**: 123094, https://doi.org/10.1016/j.watres.2025.123094.

Paerl H W, Otten T G. 2013. Harmful cyanobacterial blooms: causes, consequences, and controls. *Microbial Ecology*, **65**(4): 995-1010, https://doi.org/10.1007/s00248-012-0159-y.

Paerl H W, Xu H, McCarthy M J et al. 2011. Controlling harmful cyanobacterial blooms in a hyper-eutrophic lake (Lake Taihu, China): the need for a dual nutrient (N & P) management strategy. *Water Research*, **45**(5): 1973-1983, https://doi.org/10.1016/j.watres.2010.09.018.

Pahlevan N, Schott J R, Franz B A et al. 2017. Landsat 8 remote sensing reflectance (R_{rs}) products: evaluations, intercomparisons, and enhancements. *Remote Sensing of Environment*, **190**: 289-301, https://doi.org/10.1016/j.rse.2016.12.030.

Pontius Jr R G, Millones M. 2011. Death to Kappa: birth of quantity disagreement and allocation disagreement for accuracy assessment. *International Journal of Remote Sensing*, **32**(15): 4407-4429, https://doi.org/10.1080/01431161.2011.552923.

Qin B Q, Xu P Z, Wu Q L et al. 2007. Environmental issues of lake Taihu, China. *Hydrobiologia*, **581**(1): 3-14, https://doi.org/10.1007/s10750-006-0521-5.

Qin B Q, Zhu G W, Gao G et al. 2010. A drinking water crisis in Lake Taihu, China: linkage to climatic variability and lake management. *Environmental Management*, **45**(1): 105-112, https://doi.org/10.1007/s00267-009-9393-6.

Reynolds C S. 2006. The Ecology of Phytoplankton. Cambridge University Press, Cambridge.

Roy D P, Kovalskyy V, Zhang H K et al. 2016. Characterization of Landsat-7 to Landsat-8 reflective wavelength and normalized difference vegetation index continuity. *Remote Sensing of Environment*, **185**: 57-70, https://doi.org/10.1016/j.rse.2015.12.024.

Roy D P, Wulder M A, Loveland T R et al. 2014. Landsat-8: science and product vision for terrestrial global change research. *Remote Sensing of Environment*, **145**: 154-172, https://doi.org/10.1016/j.rse.2014.02.001.

Scheffer M, Carpenter S, Foley J A et al. 2001. Catastrophic shifts in ecosystems. *Nature*, **413**(6856): 591-596, https://doi.org/10.1038/35098000.

Scheffer M, Hosper S H, Meijer M L et al. 1993. Alternative equilibria in shallow lakes. *Trends in Ecology & Evolution*, **8**(8): 275-279, https://doi.org/10.1016/0169-5347(93)90254-M.

Shi K, Zhang Y L, Xu H et al. 2015. Long-term satellite observations of microcystin concentrations in Lake Taihu during cyanobacterial bloom periods. *Environmental Science & Technology*, **49**(11): 6448-6456, https://doi.org/10.1021/es505901a.

Wang Y J, Cao X Y, Zeng J et al. 2020. Distinct shifts in bacterioplankton community composition and functional gene structure between macrophyte- and phytoplankton-dominated regimes in a large shallow lake. *Limnology and Oceanography*, **65**(S1): S208-S219, https://doi.org/10.1002/lno.11373.

Wu T F, Qin B Q, Brookes J D et al. 2015. The influence of changes in wind patterns on the areal extension of surface cyanobacterial blooms in a large shallow lake in China. *Science of the Total Environment*, **518**-**519**: 24-30, https://doi.org/10.1016/j.scitotenv.2015.02.095.

Xie D, Yu D, You W H et al. 2013. Algae mediate submerged macrophyte response to nutrient and dissolved inorganic carbon loading: a mesocosm study on different species. *Chemosphere*, **93**(7): 1301-1308, https://doi.org/10.1016/j.chemosphere.2013.07.008.

Xiong J F, Lin C, Cao Z G et al. 2022. Development of remote sensing algorithm for total phosphorus concentration in eutrophic lakes: conventional or machine learning? *Water Research*, **215**: 118213, https://doi.org/10.1016/j.watres.2022.118213.

Xue K, Ma R H, Shen M et al. 2023. Horizontal and vertical migration of cyanobacterial blooms in two eutrophic lakes observed from the GOCI satellite. *Water Research*, **240**: 120099, https://doi.org/10.1016/j.watres.2023.120099.

Yang J Z C, Luo J H, Lu L R et al. 2021. Changes in aquatic vegetation communities based on satellite images before and after pen aquaculture removal in East Lake Taihu. *Journal of Lake Sciences*, **33**(2): 507-517. (in Chinese with English abstract)

Zeng L, He F, Dai Z G et al. 2017. Effect of submerged macrophyte restoration on improving aquatic ecosystem in a subtropical, shallow lake. *Ecological Engineering*, **106**: 578-587, https://doi.org/10.1016/j.ecoleng.2017.05.018.

Zhang M, Yang Z, Shi X G. 2019. Expansion and drivers of cyanobacterial blooms in Lake Taihu. *Journal of Lake Sciences*, **31**(2): 336-344, (in Chinese with English abstract).

Zhang Y L, Liu X H, Qin B Q et al. 2016. Aquatic vegetation in response to increased eutrophication and degraded light climate in Eastern Lake Taihu: implications for lake ecological restoration. *Scientific Reports*, **6**(1): 23867, https://doi.org/10.1038/srep23867.

Zhang Z, Zhang M, Xiao W et al. 2018. Analysis of temporal and spatial variations in NDVI of aquatic vegetation in Lake Taihu. *Journal of Remote Sensing*, **22**(2): 324-334. (in Chinese with English abstract)

Zhao D H, Jiang H, Yang T W et al. 2012. Remote sensing of aquatic vegetation distribution in Taihu Lake using an improved classification tree with modified thresholds. *Journal of Environmental Management*, **95**(1): 98-107, https://doi.org/10.1016/j.jenvman.2011.10.007.

Zhao D H, Lv M T, Jiang H et al. 2013. Spatio-temporal variability of aquatic vegetation in Taihu Lake over the past 30 years. *PLoS One*, **8**(6): e66365, https://doi.org/10.1371/journal.pone.0066365.

Zhao K, Li Z G, Wei H N et al. 2015. The distribution of aquatic vegetation in Gonghu Bay, Lake Taihu, 2012. *Journal of Lake Sciences*, **27**(3): 421-428. (in Chinese with English abstract)

Zhao K, Zhou Y F, Jiang Z L et al. 2017. Changes of aquatic vegetation in Lake Taihu since 1960*s*. *Journal of Lake Sciences*, **29**(2): 351-362. (in Chinese with English abstract)

Zhu M Y, Paerl H W, Zhu G W et al. 2014. The role of tropical cyclones in stimulating cyanobacterial (*Microcystis* spp.) blooms in hypertrophic Lake Taihu, China. *Harmful Algae*, **39**: 310-321, https://doi.org/10.1016/j.hal.2014.09.003.

Zhu M Y, Zhu G W, Nurminen L et al. 2015. The influence of macrophytes on sediment resuspension and the effect of associated nutrients in a shallow and large lake (Lake Taihu, China). *PLoS One*, **10**(6): e0127915, https://doi.org/10.1371/journal.pone.0127915.